

Shielding islets with human amniotic epithelial cells enhances islet engraftment and revascularization in a murine diabetes model

Fanny Lebreton¹  | Kevin Bellofatto¹ | Charles H. Wassmer¹ | Lisa Perez¹ |
 Vanessa Lavallard¹  | Géraldine Parnaud¹ | David Cottet-Dumoulin¹ | Julie Kerr-Conte²  |
 François Pattou²  | Domenico Bosco¹ | Véronique Othenin-Girard³ |
 Begoña Martinez de Tejada^{3,4} | Ekaterine Berishvili^{1,5} 

¹Cell Isolation and Transplantation Center, Department of Surgery, Faculty Diabetes Center, Geneva University Hospitals and University of Geneva, Geneva, Switzerland

²INSERM U1190, Translational Research for Diabetes, University of Lille, France

³Department of Pediatrics, Gynecology and Obstetrics, Geneva University Hospitals, Geneva, Switzerland

⁴Faculty of Medicine, University of Geneva, Switzerland

⁵Institute of Medical Research, Ilia State University, Tbilisi, Georgia

Correspondence

Ekaterine Berishvili
 Email: Ekaterine.Berishvili@unige.ch

Funding information

European Foundation for the Study of Diabetes; Swiss National Science Foundation, Grant/Award Number: 310030_173138; Juvenile Diabetes Research Foundation, Grant/Award Number: 31-2012-783

Hypoxia is a major cause of considerable islet loss during the early posttransplant period. Here, we investigate whether shielding islets with human amniotic epithelial cells (hAECs), which possess anti-inflammatory and regenerative properties, improves islet engraftment and survival. Shielded islets were generated on agarose microwells by mixing rat islets (RIs) or human islets (HI) and hAECs (100 hAECs/IEQ). Islet secretory function and viability were assessed after culture in hypoxia (1% O₂) or normoxia (21% O₂) in vitro. In vivo function was evaluated after transplant under the kidney capsule of diabetic immunodeficient mice. Graft morphology and vascularization were evaluated by immunohistochemistry. Both shielded RIs and HIs show higher viability and increased glucose-stimulated insulin secretion after exposure to hypoxia in vitro compared with control islets. Transplant of shielded islets results in considerably earlier normoglycemia and vascularization, an enhanced glucose tolerance, and a higher β cell mass. Our results show that hAECs have a clear cytoprotective effect against hypoxic damages in vitro. This strategy improves β cell mass engraftment and islet revascularization, leading to an improved capacity of islets to reverse hyperglycemia, and could be rapidly applicable in the clinical situation seeing that the modification to HIs are minor.

KEYWORDS

basic (laboratory) research/science, diabetes: type 1, islet transplantation, islets of Langerhans, regenerative medicine, stem cells, tissue/organ engineering, translational research/science

Abbreviations: ANGPT1, angiopoietin 1; ATMP, advanced therapy medicinal product; BSA, bovine serum albumin; CB17-SCID, CB-17/1cr-Prkdc^{scid}/Rj; CCER, Commission Cantonale d'Ethique de la Recherche; CMRL, Connaught Medical Research Laboratories medium; CTT, cell and tissue-based therapeutics; DAPI, 4',6-diamidino-2-phénylindole; EGF, epidermal growth factor; FBS, fetal bovine serum; FDA, fluorescein diacetate; FITC, fluorescein isothiocyanate; GSIS, glucose-stimulated insulin secretion; hAEC, human amniotic epithelial cell; HBSS, Hanks' balanced salt solution; HI, human islet; HIF-1 α , hypoxia-inducible factor 1-alpha; IC-hAEC, insulin-secreting organoids combining dissociated islet cells with hAECs; IEQ, islet equivalent; IPGTT, intraperitoneal glucose tolerance test; KRB, Krebs' Ringer buffer; MEM-NEAA, minimum essential medium nonessential amino acids; MSC, mesenchymal stem cell; NOD-Rag1^{null}, B6.129S7-Rag1^{tm1Mom/J}; PDGF-B, platelet-derived growth factor subunit b; PFA, paraformaldehyde; PI, propidium iodide; PP, pancreatic polypeptide; RI, rat islet; SI, stimulation index; VEGF-A, vascular endothelial growth factor A.

Fanny Lebreton and Kevin Bellofatto contributed equally to the article.

1 | INTRODUCTION

Despite remarkable progress made during the past decades, clinical islet transplant remains suboptimal in terms of engraftment and long-term survival. A large proportion of islets is lost in the immediate posttransplant period, and further cell loss occurs in the following revascularization period. Consequently, islets from several donors are needed to achieve engraftment of what is considered to be a marginal islet mass, ensuring adequate endocrine function, but sometimes also leading to β cell exhaustion in the long term.^{1,2} Major causes of early graft loss include the inflammatory reaction at the transplant site and the disruption of the islet microvasculature during the isolation process.^{1,3,4} Full revascularization of transplanted islets takes between 10 and 24 days.⁵ In the meantime, oxygen and nutrients are supplied to the islet core only via passive diffusion, resulting in hypoxia and nutrient deprivation, and thus in cell death and impairment of long-term engraftment.⁶

New strategies aimed at both accelerating revascularization of the graft and reducing inflammatory injury are of crucial importance to improve long-term success of islet transplant.

Several groups have reported beneficial effects of cotransplant of islets of Langerhans and other cell types, for example, mesenchymal stromal cells (MSCs) or parathyroid cells. Islet engraftment, endocrine function, and islet graft survival were enhanced through a number of mechanisms, such as maintenance of islet structural organization and enhancement of revascularization.⁷⁻¹⁰

Our approach takes advantage of the characteristics of human amniotic epithelial cells (hAECs). hAECs have immunomodulatory properties and stem cell features, such as pluripotency, and are easily accessible in high amounts without ethical constraints.¹¹ Relevant to this study, they also secrete a number of angiogenic and anti-inflammatory growth factors.¹² These properties make hAECs attractive for combination with islet grafts, with the aim to improve engraftment and revascularization. We have recently shown that combining hAECs with dissociated islet cells in insulin-secreting organoids protects islet cells against hypoxia-induced damage *in vitro* and improves β cell engraftment and vascularization after transplant in diabetic immunodeficient mice.¹³ Despite the proven advantages of generating multicellular islet spheroids in terms of functionality, viability, and engraftment, this approach requires dissociation of isolated islets, which may induce a loss of β cell mass.¹⁴⁻¹⁶ A simpler method, avoiding manipulation of the intact islets, would circumvent the drawbacks of a classification as an advanced therapy medicinal product (ATMP).

In the present study, we have designed a hybrid construct by shielding native islets with a layer of hAECs and demonstrated that cotransplant of hAECs with islets improves blood glucose control in diabetic mice.

2 | MATERIALS AND METHODS

2.1 | Animals

All experiments were performed in compliance with the rules of Geneva veterinary authorities and were approved by University of Geneva Institutional Animal Care and Use Committee. Ten-week-old

male Lewis rats (LEW/OrlRj from Janvier Labs, Le Genest St-Isle, France) were used for pancreatic islet isolation. Six- to 8-week-old male CB-17/1cr-Prkdc^{scid}/Rj (abbreviated CB17-SCID, from Janvier Labs) or B6.129S7-Rag1^{tm1Mom}/J (abbreviated NOD-Rag1^{null} bred at Charles River Laboratories, Saint-Germain-Nuelles, France) mice were used for transplant experiments. All animals were kept under conventional housing conditions with free access to food and water before experiments.

2.2 | Human tissues

Studies involving human tissues were approved by the state of Geneva Ethics Committee (Commission Cantonale d'Ethique de la Recherche [CCER]), in compliance with the Swiss Human Research Act (810.30). Amniotic membranes were harvested from term healthy placentae of woman undergoing elective cesarean section at the Geneva University Hospitals, under CCER protocol 2017-00101. Human pancreatic islets isolated from brain-dead multiorgan donors were obtained from the Cell Isolation and Transplantation Center of the Geneva University Hospitals and University of Lille France in the context of the ECIT grant (JDRF). Human islet donor characteristics are listed in Table S1. The use of human islets for research was approved by CCER protocol 2016-01979.

2.3 | Isolation of hAECs

hAECs were isolated, cultured, and characterized by flow cytometry as previously described.^{11,13} hAECs were harvested after 5-7 days at 80% confluence via mild trypsinization (0.05% trypsin/EDTA) and were cryopreserved in liquid nitrogen for later use. hAECs derived from 8 different human placentae were used. In particular, cells obtained from 3 distinct preparations were used for the *in vitro* experiments, and cells from all 8 preparations for the *in vivo* studies.

2.4 | Islet isolation, generation of shielded islets, and culture

2.4.1 | Human islet isolation and culture

Before use in experiments, human islets from 4 distinct human preparations were cultured in CMRL 1066 medium (Sigma-Aldrich, Buchs, Switzerland) containing 5.6 mmol/L glucose and supplemented with 100 U/mL Penicillin and 0.1 mg/mL streptomycin, 25 mmol/L HEPES (ThermoFisher Scientific, Reinach, Switzerland), and 10% FBS (hereafter referred to as human islet complete medium) for 2-6 days.

2.4.2 | Rat islet isolation and culture

Rat pancreatic islets were isolated as previously described^{13,17} and cultured in DMEM supplemented with 10% (v/v) FBS, 1 mmol/L sodium

pyruvate, 11 mmol/L glucose (Bichsel, Interlaken, Switzerland), 0.05 mmol/L 2-mercaptoethanol, 2 mmol/L L-glutamine, 100 U/mL penicillin, and 0.1 mg/mL streptomycin (hereafter referred to as rat islet complete medium).

2.4.3 | Generation of shielded islets

Shielded islets were generated on 3-dimensional (3D) agarose-patterned microwells, using 3D Petri Dish (Microtissues Inc., Sigma-Aldrich) with 256 microwells (400- μ m diameter and 800- μ m depth). Handpicked islets were mixed with hAECs at a ratio of 100 hAECs per islet equivalent (IEQ) and seeded onto the agarose casts (256 IEQ per cast). The 1:100 islet:hAEC ratio was selected according to performance in glucose-stimulated insulin release assays (data not shown). To ensure homogeneous distribution of constructs, the microwells were placed on a plate shaker at 200 rpm for 30 minutes and cultured for 6 days. Cell aggregation was monitored daily. Shielded islets were retrieved from the agarose casts by flipping the casts upside down in the plate, before centrifugation at 300g for 2 minutes. Islet diameter was calculated by analyzing light microscopy images with ImageJ software (National Institutes of Health, Bethesda, MD).

2.5 | Shielded islet cell aggregation and 3D organization assessment

hAECs were labeled with CellTracker DiO (ThermoFisher Scientific) fluorescent dye, according to the manufacturer's protocol, before seeding. Aggregation of labeled cells around the islets was monitored using an epifluorescent microscope (DMi8 manual microscope; Leica Microsystems, Heerbrugg, Switzerland) for up to 6 days.

After 6 days of culture, shielded islets were removed from the microwells and processed for immunofluorescent histology as previously described¹³ with a primary antibody against insulin (1:100 dilution; DakoCytomation, Baar, Switzerland) and an anti-guinea pig Alexa 555 secondary antibody (1:300 dilution, ThermoFisher Scientific), followed by nuclear counterstaining using Hoechst (1:1000 dilution, Sigma-Aldrich). Stained shielded islets were transferred into microscopy culture chambers (Ibidi, Planegg, Germany) and subjected to optical z-stacking with 2.5- μ m increments using a spectral confocal microscope (Nikon A1R; Nikon Imaging, Egg, Switzerland). The resulting z-series were processed into 3D representations using NIS-Elements Imaging Software (version 4.20.00 Build 972; Nikon Imaging).

2.6 | In vitro viability and functional assessment

To assess whether hAEC shielding confers protection to the islet under ischemic conditions, shielded islets and control islets were cultured for 16 hours (rat) or 24 hours (human) under hypoxic culture conditions in a humidified atmosphere. To achieve this, the incubator was connected to a nitrogen supply to adjust the nitrogen:oxygen

ratio (1% oxygen, 5% CO₂, 94% nitrogen, 37°C). Islet viability was evaluated by fluorescein diacetate (FDA) and propidium iodide (PI) staining. At least 50 control or shielded islets per condition were analyzed to quantify the proportion of FDA and PI positive cells (ie, viable and dead cells, respectively).

Insulin secretory function of control and shielded islets was evaluated by distributing 50 IEQ in duplicate for each condition in Millicell culture inserts (Merck, Schaffhausen, Switzerland) in a 24-well culture plate. They were first preincubated in Krebs-Ringer buffered HEPES (pH 7.4) with 0.1% (w/v) BSA (KRB) for 1 hour at 37°C and then successively incubated for 1 hour at 37°C in KRB solutions containing glucose at low (2.8 mmol/L) or high (16.7 mmol/L) concentration. Finally, islets were incubated 1 hour at room temperature in an acid-ethanol solution to lysate cell membranes and extract total insulin content. Insulin concentration in supernatants was determined by ELISA (Mercodia, Uppsala, Sweden) and normalized to the total insulin content. The stimulation index (SI), defined as the ratio of the concentration of insulin secreted in high-glucose solution to the concentration of insulin secreted in low-glucose solution, was used as an indicator of islet responsiveness to glucose.

2.7 | Diabetes induction, xenogeneic islet transplant, and in vivo functional assessment of the graft

One week before transplant, mice were injected intraperitoneally with streptozotocin (Sigma-Aldrich) at the dose of 216 mg/kg. Nonfasting blood glucose levels were then checked daily from blood samples taken from the tail using a portable glucometer (Freestyle Precision; Abbott Diabetes Care, Baar, Switzerland). Only mice with blood glucose levels >18 mmol/L for 3 consecutive days were used in transplant experiments.

After 3 days of culture, islets (275 IEQ in rat islet experiments, 2000 IEQ in human islet experiments) were packed in PE50 tubing (PhyMep, Paris, France) and transplanted under the kidney capsule of diabetic mice by using a screw-drive syringe (Hamilton, Reno, NV). Nonfasting blood glucose levels were measured daily during the first week following transplant and then twice a week. Euglycemia was defined as blood glucose levels <11.1 mmol/L.

Intraperitoneal glucose tolerance test (IPGTT) was performed to assess graft responsiveness to glucose. Mice were fasted for 6 hours before being injected intraperitoneally with 2 g/kg body weight glucose and blood glucose was measured at 0, 15, 30, 45, 60, and 120 minutes.

Graft-bearing kidneys were removed at 2, 4, or 8 weeks to exclude residual function of the native pancreas and for histology. Blood glucose levels were monitored to verify loss of euglycemia.

2.8 | Histological analysis

Islets were fixed in 4% (w/v) PFA for 30 minutes at room temperature, washed 3 times in PBS (Sigma-Aldrich) and dehydrated before being embedded in agarose (Histogel; ThermoFisher Scientific) and paraffin.

Retrieved grafts were fixed in 4% (w/v) PFA and embedded in paraffin. Tissue or islet samples were processed for immunofluorescent histology as published¹³ and stained with primary antibodies against insulin (1:100; DakoCytomation), glucagon (1:4000; Sigma-Aldrich), somatostatin (1:100; DakoCytomation), pancreatic polypeptide (1:100; DakoCytomation), CD34 (1:2500; Abcam, Cambridge, UK), and Ki67 (1:100; GeneTex Inc., Alton Pkwy Irvine, CA), followed by staining with goat anti-mouse, anti-rabbit, anti-guinea pig Alexa555-conjugated (1:300; ThermoFisher Scientific) or goat anti-guinea pig FITC-conjugated (1:200; Jackson ImmunoResearch Laboratories, Ely, UK) secondary antibodies. Histological slides were mounted with aqueous mounting medium containing DAPI (Fluoroshield Mounting Medium with DAPI, Abcam) for nuclear counterstaining. Images of stained sections were captured using a Zeiss Axioscan.Z1 slide scanner (Zeiss, Feldbach, Germany) for automated imaging.

Morphometry and fluorescent analyses were performed on every fifth section (i.e., 20%) of the total graft ($n = 3$ in each group) stained with anti-insulin and anti-CD34 antibodies. The entire sections were captured using a Zeiss Axioscan.Z1 slide scanner (Zeiss) for automated imaging. Insulin⁺ areas and CD34⁺ areas were measured semiautomatically by Zen 2.3 Blue Edition software (version 2.3.60.1000; Zeiss).

2.9 | Statistical analysis

Continuous and categorical variables are presented as mean \pm SD. Comparisons between groups were performed with unpaired 2-tailed Student's *t* test or 1-way/2-way ANOVA with Tukey post-hoc test wherever appropriate. The log-rank (Mantel-Cox) test was used to compare the cumulative number of animals reaching normoglycemia. All statistical analyses were performed with Prism software 7.02 (GraphPad, La Jolla, CA), and $P < .05$ was considered statistically significant.

3 | RESULTS

3.1 | Engineering of shielded islets

Figure 1A describes the procedure used to generate shielded islets in agarose micromolds. hAEC aggregation around islets was complete within 2 days (Figure 1B). Confocal laser scanning microscopy (Figure 2) and the corresponding 3D reconstruction (Video S1) show a uniform hAEC layer around the human islets. Immunohistochemical analysis reveals that the 4 endocrine cell types were present in the shielded islets (Figure S1).

Although contradictory evidence was recently published,¹⁸ it has been reported that islets of small diameter perform better than larger islets.^{19,20} To ensure that the expected higher performances of shielded islets compared with control islets resulted from a beneficial effect of hAECs and were not due to the selection of small islets in the shielding procedure, *in vitro* function of small ($\leq 150 \mu\text{m}$)

uncovered islets and control islets of mixed sizes were analyzed and no difference in the secretory function was observed between small or mixed islets (stimulation index [SI]: 2.7 ± 0.9 vs 2.3 ± 0.6 , $P = .9$, not shown). Average diameter of shielded and control islets before use in experiments was $161.3 \pm 26.5 \mu\text{m}$ and $168 \pm 42.5 \mu\text{m}$, respectively, in the rat experiments ($P = .3$) and $121.8 \pm 42.5 \mu\text{m}$ and $131.8 \pm 36.9 \mu\text{m}$, respectively, in the human experiments ($P = .09$).

3.2 | In vitro viability and functionality of shielded islets

To assess the ability of hAECs to exhibit cytoprotective properties under ischemic stress, both control and shielded islets were exposed to hypoxic culture conditions (1% O₂/5% CO₂ at 37°C).

Although exposure to hypoxia caused a pronounced cell death in control rat islets, shielded rat islets showed a lower number of dead cells (Figure 3A, C). Under normoxic conditions, the secretory function of shielded islets was significantly higher than in control islets (SI = 6.9 ± 1.4 vs 2.1 ± 0.8 , $P = .006$; Figure 3E, Figure S3). Exposure to hypoxic culture conditions for 16 hours induced a drastic impairment of insulin secretion of control islets compared with normoxia (SI = 0.8 ± 0.2 vs 2.1 ± 0.8 , $P = .03$), demonstrating a complete loss of responsiveness to glucose. In contrast, shielded islets remained responsive to glucose stimulation even after hypoxia exposure (SI = 2.1 ± 0.8 vs 1.6 ± 0.5 , $P = \text{ns}$; Figure 3E). Experiments performed on human islets confirmed the cytoprotective effect conferred by the hAEC shielding under hypoxic conditions (Figure 3D). The shielding strategy also allowed to abolish the effect of hypoxia on rat islet *in vitro* function and human islet viability. Only a slight difference persisted when comparing the viability of control rat islets under normoxia with shielded rat islets under hypoxia (Figure 3C).

3.3 | Marginal mass transplant of shielded islets improves islet cell function and glycemic control *in vivo*

To assess whether the hAEC protective layer could improve islet engraftment and diabetes reversal, diabetic NOD-*Rag1*^{null} mice were transplanted with a marginal mass of 275 control (RI group, $n = 12$) or shielded (RI + hAEC group, $n = 11$) rat IEQ. Mice transplanted with shielded islets showed better glycemic control over time compared with the control group (Figure 4A, $P = .005$). Graft retrieval after 60 days caused an increase in blood glucose levels in both groups, confirming that transplanted islets were responsible for diabetes reversal. The cumulative percentage of animals reaching normoglycemia in the RI + hAEC group was 92.3% (10/11 mice) versus 41.7% in the RI group (5/12 mice, $\chi^2 = 7.196$, $P = .007$), with a median time to normoglycemia of 2 days in the RI + hAEC group versus >30 days in the RI group (Figure 4B). The average nonfasting blood glucose levels of mice in the RI + hAEC group were significantly lower than those of mice in the RI group, at 2 weeks ($9.1 \pm 5.2 \text{ mmol/L}$, $n = 11$

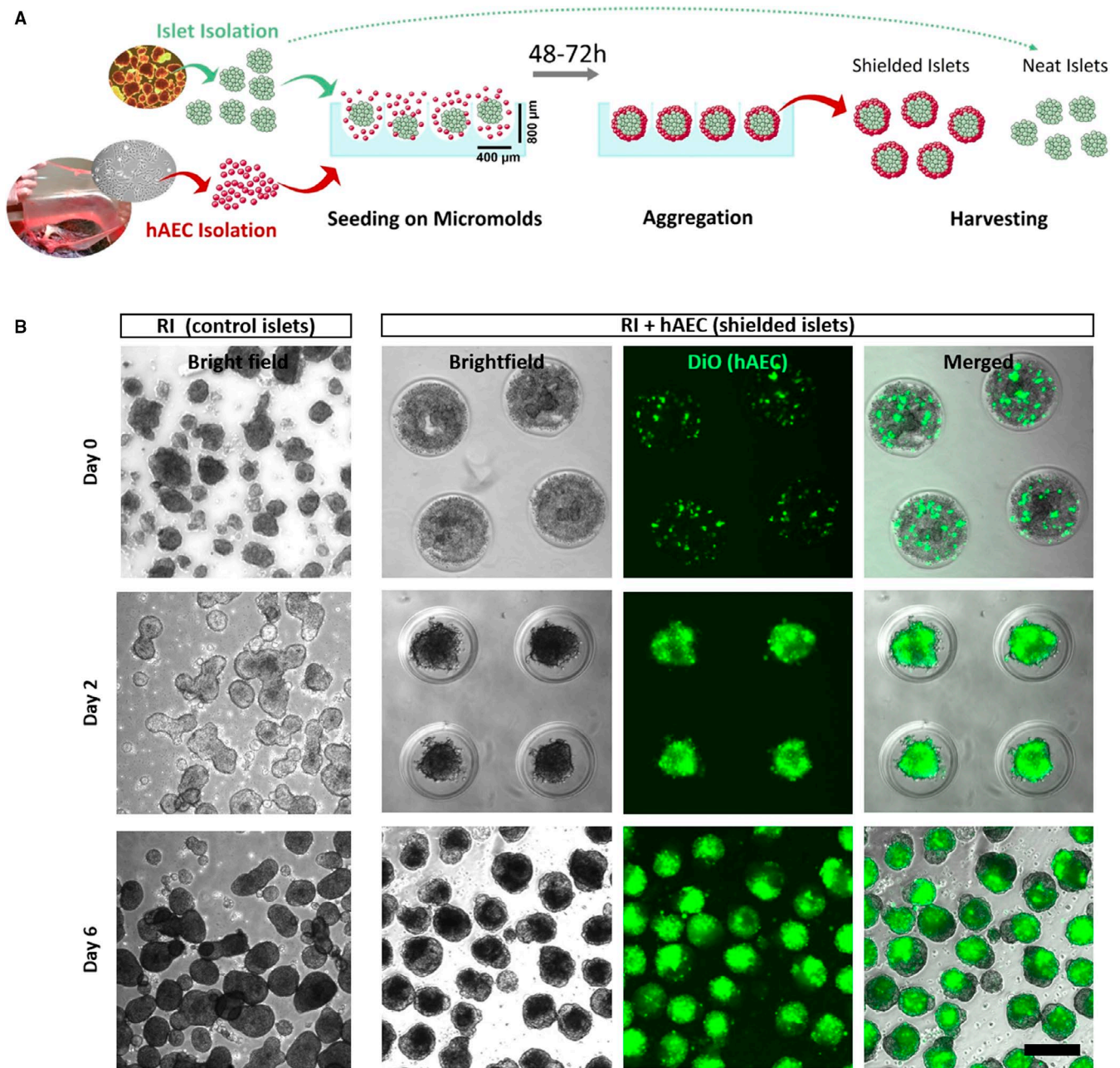


FIGURE 1 Engineering of shielded islets. **A**, Schematic representation of shielded islet formation protocol: intact islets were mixed with labeled hAECs before seeding on agarose microwells and were cultured for several days before harvesting. **B**, Brightfield and corresponding fluorescence images of control (RI) or shielded (RI + hAEC) rat islets on microwells at day 0 and day 2 and after harvesting at day 6. Scale bar = 250 μ m

and 17.0 ± 10.8 mmol/L, $n = 12$, respectively, $P = .038$) posttransplant (Figure 4C). To evaluate the functionality of transplanted islets in vivo, IPGTT was performed at 2 months after transplant. Mice in the RI group showed pathological responses similar to those of diabetic animals. In contrast, RI + hAEC-transplanted animals had a significantly different glucose clearance, resembling that of nondiabetic control mice (Figure 4D, $P < .0001$, $n = 3$ mice per group). Area under the curve was significantly lower in the RI + hAEC than in the RI group (Figure 5E; 719.8 ± 259.2 vs 2634.0 ± 523.7 , $P = .0005$).

Transplant of 2000 control (HI) or shielded (HI + hAEC) human IEQ in diabetic SCID mice produced similar results, with a better

glycemic control over time in the shielded islet groups compared with the control group (Figure 5A, $P < .0001$). The cumulative percentage of animals reaching normoglycemia in the HI + hAEC group was 71.4% (5/7 mice) versus 37.5% in the HI group (3/8 mice, $\chi^2 = 1.842$, $P = .1748$), with a median time to normoglycemia of 7 days in the HI + hAEC group versus >40 days in the HI group (Figure 5B). The average nonfasting blood glucose levels of mice in the HI + hAEC group were significantly lower than those of mice in the HI group, both at 2 weeks (9.3 ± 3.2 mmol/L, $n = 7$ and 16.9 ± 9.8 mmol/L, $n = 8$, respectively, $P = .036$) and 1 month (8.2 ± 3.7 mmol/L, $n = 7$ and 18.5 ± 4.0 mmol/L, $n = 8$, respectively, $P = .037$) posttransplant

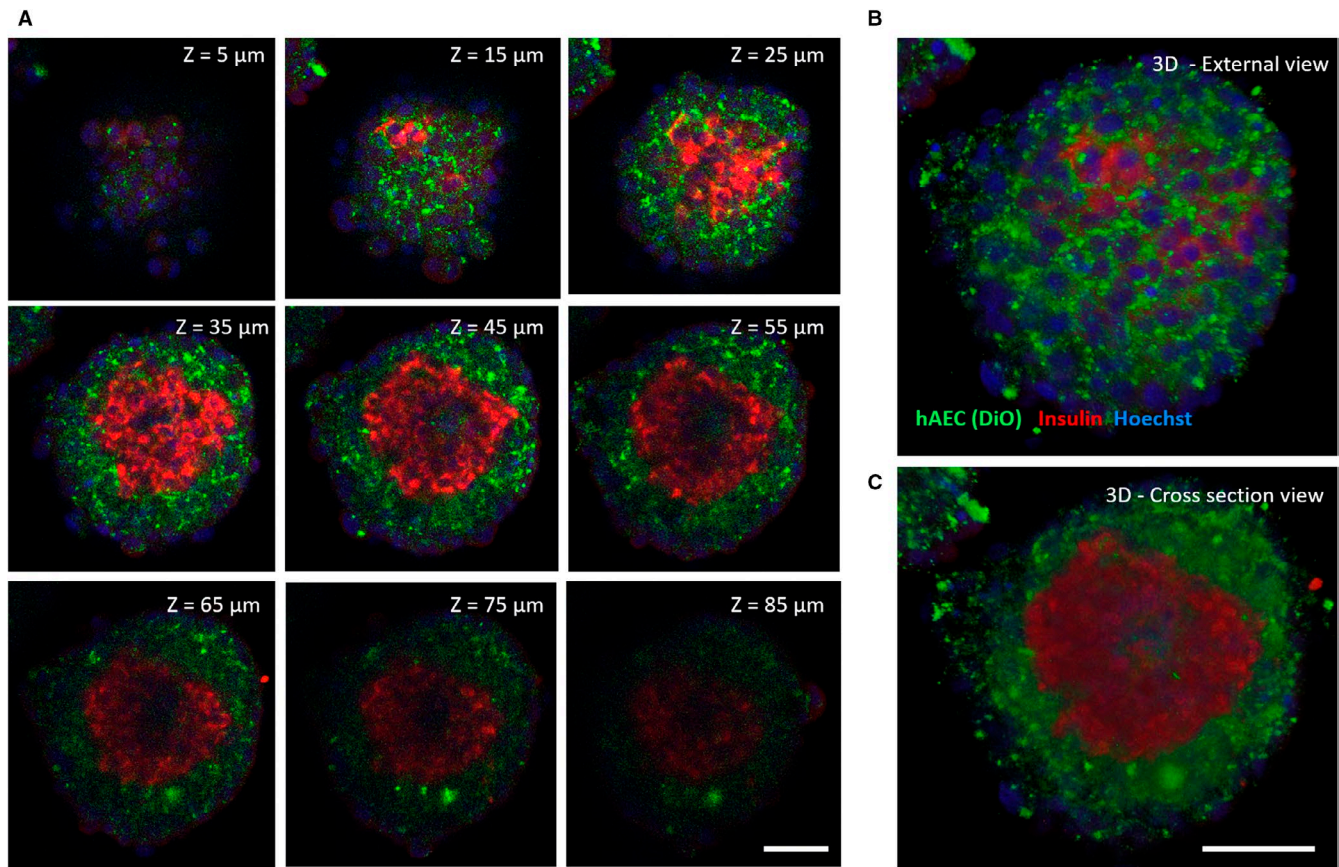


FIGURE 2 Morphological characterization of shielded human islets in vitro. A, Spectral confocal z-stacking pictures of a shielded islet in whole mount, showing the islet (insulin staining in red) covered by a layer of hAECs (DiO staining in green), and the corresponding 3D reconstructions observed from the external view (B) or a cross-sectional view (C). Scale bars = 50 μ m

(Figure 5C). This was in line with the average serum C-peptide levels at 1 month posttransplant of 3367 ± 366.3 pmol/L in the HI + hAEC group, significantly higher than the 1133.0 ± 272.7 pmol/L in the HI group (Figure 5D, $P = .0004$).

During IPGTT performed at 2 months HI + hAEC-transplanted animals showed a better glucose clearance, with an area under the curve significantly lower than that of the HI group (Figure 5E, $P = .003$).

3.4 | Shielding human islets with hAEC enhances graft revascularization

Graft-bearing kidneys were removed at >8 weeks after transplant and processed for histology in order to assess engraftment and vascularization. Figure 6A shows a higher insulin-positive area per field in the HI + hAEC group compared with the HI group ($72.2 \pm 5.6\%$ vs $49.0 \pm 7.2\%$, $P < .0001$), demonstrating the enhanced engraftment of shielded islets. No difference was observed in the density of the other endocrine cell types in the grafts, except for the pancreatic polypeptide positive cells, which were more present in the HI + hAEC group (675.7 ± 361.4) compared with the HI group (337.1 ± 135.0 , $P = .006$, Figure 6B). Vascularization was investigated using immunostaining against CD34 in control and shielded

human islet transplants. As shown in Figure 6C, higher CD34 staining was observed in HI + hAEC group compared with the HI group. Quantification reveals a 3-fold increase of CD34⁺ cells in the HI + hAEC group (1596.0 ± 745.5) compared with the HI group (690.0 ± 664.8 , $P = .0004$). Investigation of vascularization in control and shielded rat islet-transplanted kidneys also showed a significantly higher amount of CD34 staining in RI + hAEC group (2487.0 ± 499.2) than in the RI group (1424.0 ± 353.1 , $P = .0002$; Figure S4). Because hAECs are expanding cells when cultured in vitro, we assessed cell proliferation in the graft using Ki67 staining; Figure S5 shows no difference between the 2 groups, demonstrating the absence of proliferating cells in the explanted grafts.

4 | DISCUSSION

In this study, we have shown that shielding islets with a layer of hAECs enhances islet secretory function and viability in vitro, in both normoxic and hypoxic conditions, and islet engraftment and function in vivo after transplant in a diabetic murine model.

The cytoprotective effects of hAECs against hypoxia-induced damage to islet cell viability and function are consistent with what we previously described in insulin-secreting organoids combining dissociated islet cells with hAECs (IC-hAEC). In this study, improved

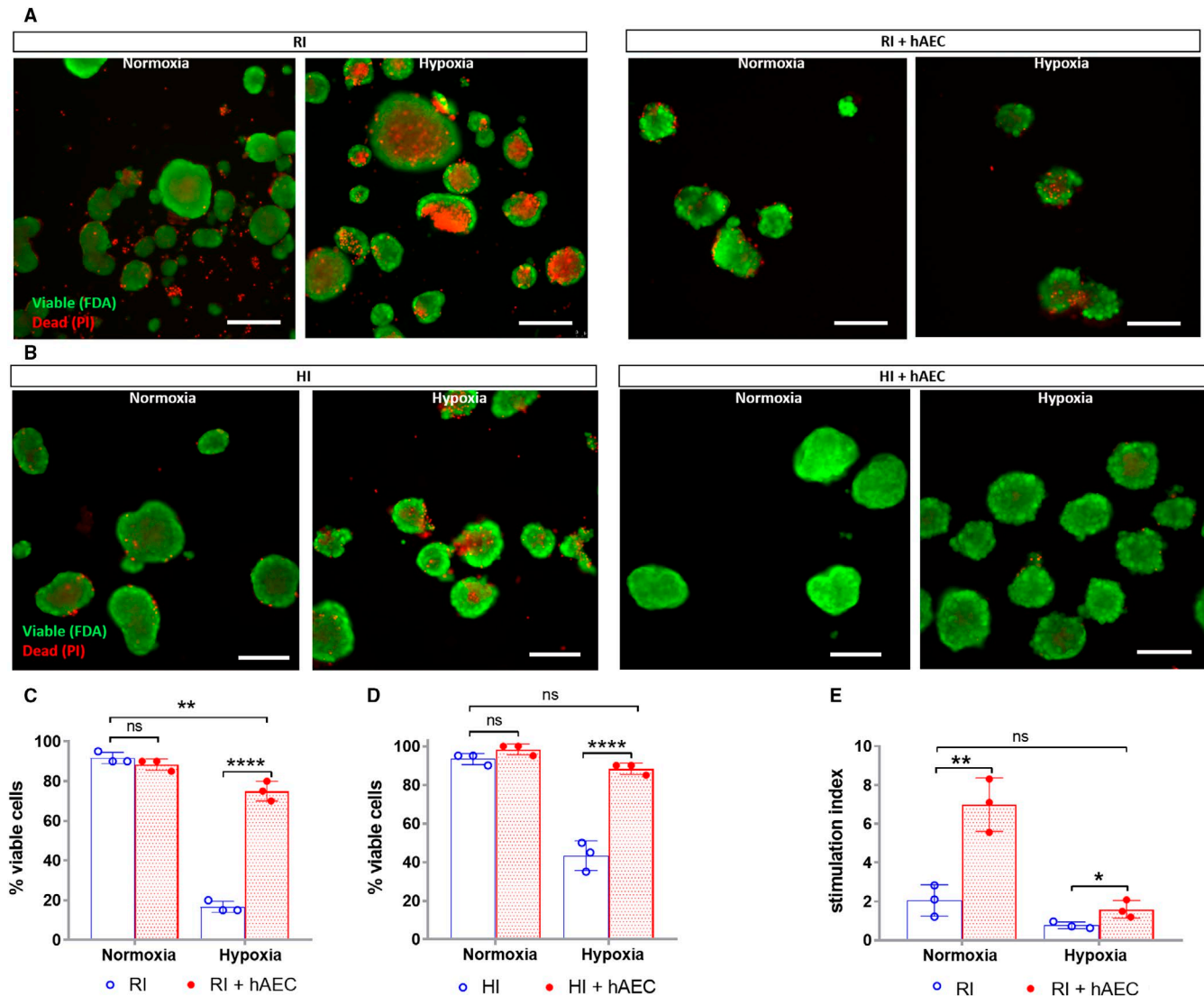


FIGURE 3 Viability and functional changes in shielded rat and human islets after a hypoxic stress in vitro. A and B, Epifluorescent images of control (RI) and shielded (RI + hAEC) rat islets (A), or control (HI) and shielded (HI + hAEC), cultured in normoxic conditions or after a 16-24 hours (respectively) of hypoxia. FDA/PI staining shows viable cells in green and dead cells in red. Scale bars = 200 μ m. C and D, Quantification of viability from FDA/PI fluorescent images. E, Stimulation index from the glucose insulin secretion test performed on control or shielded islets exposed to normoxic or hypoxic culture conditions. * $P \leq .05$, ** $P \leq .01$, **** $P < .0001$, 2-tailed unpaired Student's *t* test, $n = 3$. All data are shown as mean \pm SD

viability and function of organoids after hypoxia were associated with the upregulation of hypoxia-inducible factor 1- α (HIF-1 α),¹³ which is involved in regulatory protection mechanisms triggered during hypoxic events.^{21,22}

One of the main causes of islet death following transplant is the lack of oxygenation and nutrient supply due to disruption of the islet intrinsic microvasculature and slow revascularization in the recipient. hAECs have been shown to promote vessel formation in vitro²³ and angiogenesis in vivo,²⁴ in correlation with the expression of numerous angiogenic factors directly involved in the revascularization process, such as vascular endothelial growth factor-A (VEGF-A), platelet-derived growth factor subunit B (PDGF-B), and angiopoietin-1 (ANGPT1).^{12,23,24} Among these factors, the VEGF family is known to stimulate the migration of

endothelial cells and improve vascular permeability.²⁵ It has been shown that a combination of VEGF-A and PDGF-B promotes islet engraftment in mice^{26,27} in extrahepatic sites. Another angiogenic factor, ANGPT1, improves islet engraftment and exerts cytoprotective effects in vivo.²⁸ The coexpression of these markers in hAECs, along with other factors proven to increase VEGF-A expression such as interleukin-6 or angiogenin,²⁹ are likely mechanisms for the improved vascularization of shielded islets grafts reported herein.

This is in line with our previous work, showing increased levels of VEGF-A expression¹³ in IC-hAEC organoids compared with controls in hypoxic conditions in vitro, as well as in IC-hAEC grafts in vivo, indicating that improved vascularization is mediated by hAECs via up-regulation of VEGF-A expression. Because VEGF-A is a target gene

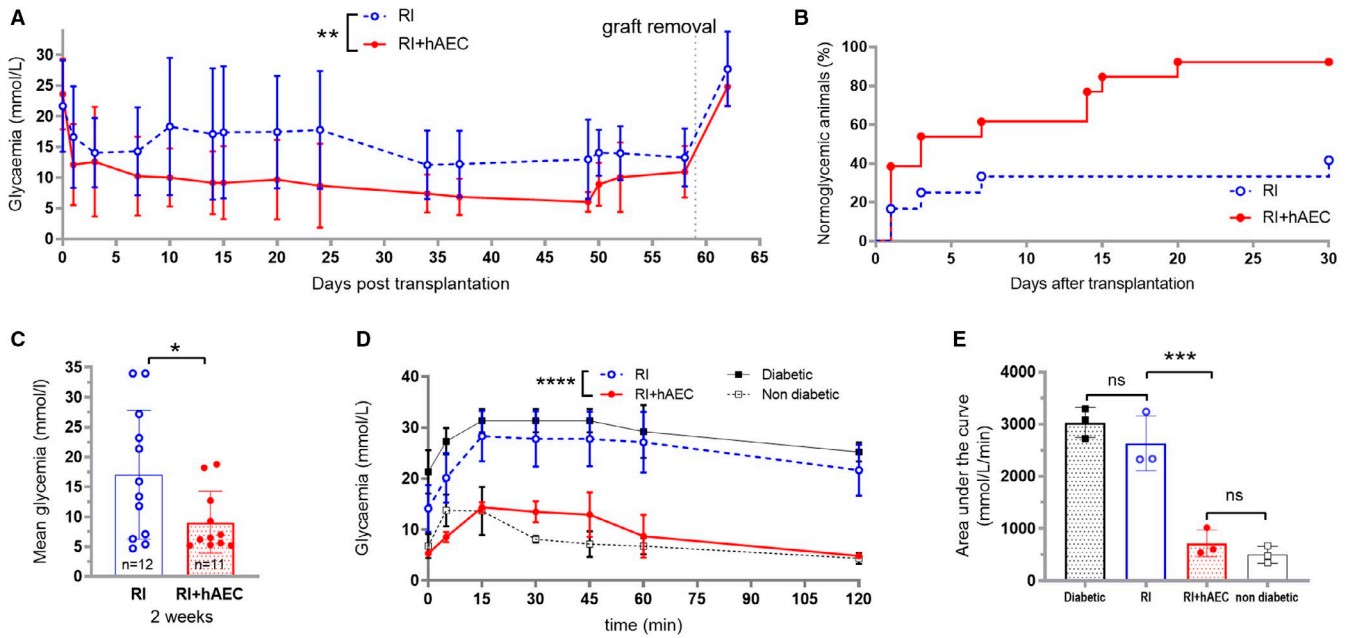


FIGURE 4 In vivo functional assessment of shielded rat islets transplanted in the diabetic immunodeficient mice. A, Blood glucose over time measured in diabetic NOD-*Rag1*^{null} mice transplanted with 275 control (RI group, blue circles n = 12 until day 15, n = 8 until day 35, n = 6 until the end of the experiment) or shielded (RI + hAEC group, red circles n = 11 until day 15, n = 7 until day 35, n = 5 until the end of the experiment) rat islets. ***P* ≤ .01, 2-tailed unpaired Student's *t* test. B, Cumulative proportion of animals normalizing blood glucose levels. C, Mean glycaemia in each group calculated at 2 weeks after transplant. **P* ≤ .05, 2-tailed unpaired Student's *t* test. D and E, Intraperitoneal glucose tolerance test conducted at 2 months (E) and the corresponding area under the curve (F). White squares: nondiabetic animals, dark squares: diabetic animals, blue circles: control islet-transplanted animals, red circles: shielded islet-transplanted animals. ****P* ≤ .001, *****P* < .0001 between RI and RI-hAEC, ANOVA with Tukey's post-hoc comparison, n = 3 per group. All data are shown as mean ± SD

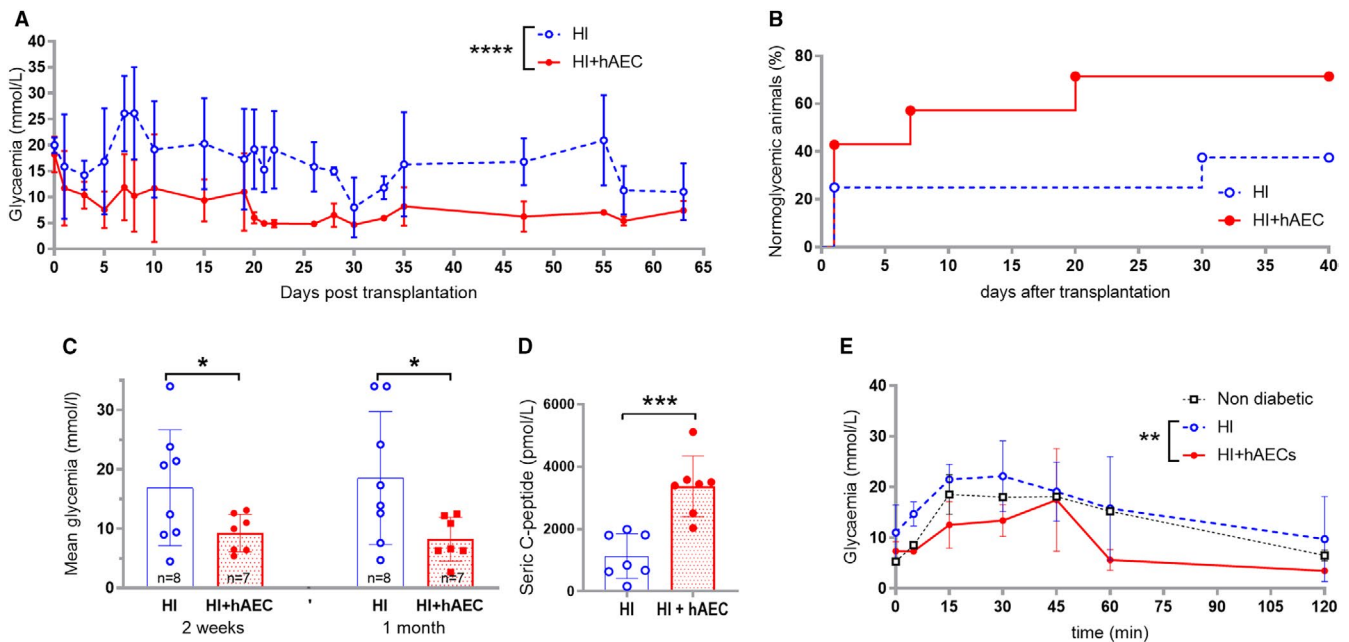


FIGURE 5 In vivo functional assessment of shielded human islets transplanted in the diabetic immunodeficient mice. A, Blood glucose over time measured in diabetic CB17-SCID mice transplanted with 2000 control (HI group, blue circles n = 8 until day 30, n = 5 until the end of the experiment) or shielded (HI + hAEC group, red circles n = 8 until day 30, n = 3 until the end of the experiment) human islets. *****P* ≤ .0001, 2-tailed unpaired Student's *t* test. B, Cumulative proportion of animals normalizing blood glucose levels. C, Mean glycaemia in each group calculated at 2 weeks (left) and 1 month (right) after transplant. **P* < .05, 2-tailed unpaired Student's *t* test. D, Fasting C-peptide levels in serum at 2 months after transplant. ****P* < .001, 2-tailed unpaired Student's *t* test, n = 7 per group. E, Intraperitoneal glucose tolerance test conducted at 2 months (white squares: nondiabetic animals, blue circles: control islet-transplanted animals, red circles: shielded islet-transplanted animals). ***P* < .001, ANOVA with Tukey's post-hoc comparison, n = 2 per group. All data are shown as mean ± SD

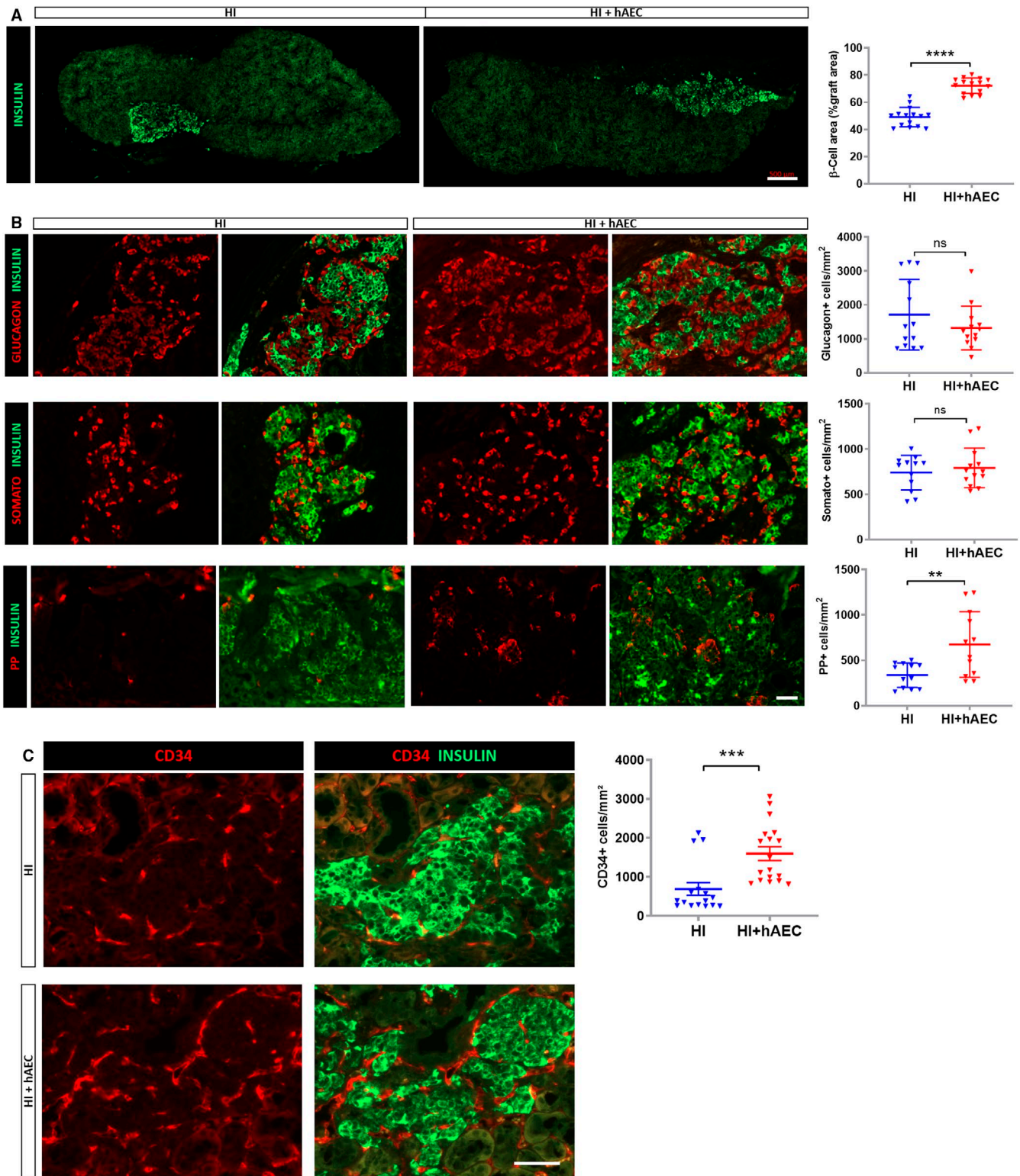


FIGURE 6 Immunohistological analysis of hormone expression and vascularization in transplanted control and shielded human islets. Graft-bearing kidneys were explanted 2 months after transplant, fixed and serial sections from three mice per group were processed for immunohistological stainings. A, Insulin-positive area and corresponding quantification expressed in percentage of insulin-positive area over total graft area. Scale bar = 500 μ m. B, Immunohistological stainings for glucagon, somatostatin (somato), and pancreatic polypeptide (PP) and their quantification for a given area expressed in number of positive cells/mm². Scale bar = 50 μ m. C, Detection and quantification of the blood vessels stained against CD34. Scale bar = 50 μ m. $**P \leq .01$, $***P < .001$, $****P \leq .0001$, 2-tailed unpaired Student's *t* test, $n = 3$ mice per group. All data are shown as mean \pm SD

of HIF-1 α , it is likely that upregulation of HIF-1 α due to early post-transplant ischemia of the islets is responsible for overexpression of VEGF-A and subsequent enhanced vascularization of the graft.²²

Protective effects of hAECs and revascularization of transplanted islets both contributed to better engraftment of shielded islets, associated with a better in vivo function and a higher rate of diabetes reversal. The better engraftment of shielded islets could also be attributed to a restored extracellular matrix microenvironment in the shielded islet group, as hAECs produce extracellular matrix proteins crucial for β cell function.^{13,30,31} The absence of Ki67 staining in the explanted grafts confirmed that the higher β cell area in the shielded islet group resulted from a better engraftment and survival rather than a proliferation of transplanted islets or hAECs. Moreover, we previously observed that hAECs were detected in the grafts until 2 weeks after transplant before decreasing overtime, showing that the beneficial effects of hAECs are provided to islets in the early posttransplant period.¹³

Several studies have explored cotransplant of stem cells (mostly mesenchymal stromal cells) with islets, leading to improved vascularization in syngeneic models.^{7,9,32} However, stem cells were transplanted as a cell suspension, implying that cells can be washed out in the portal blood flow before engrafting or engraft far from the islets during intraportal infusion. In contrast, our shielding strategy favors proximity and easier diffusion of factors secreted by hAECs to the islets. The proangiogenic capacities of hAECs could also allow exploring extrahepatic transplant sites where islet engraftment is currently hampered by a poor vascularization potential. Indeed, recent transplant studies in the subcutaneous space have shown improved engraftment of islets cotransplanted with vascular endothelial progenitor cells from the parathyroid gland, which are known to secrete angiogenic factors and to promote revascularization.^{8,10}

One remarkable finding of this study is the consistency of hAECs' beneficial effects across species, as results obtained in rat islets were confirmed using human islets. This is of crucial importance considering the multiple morphological or functional differences that exists between rodent and human islets,³³⁻³⁵ and we can thus assume that the protection provided to human islets by our shielding strategy could also be provided in the context of clinical transplant in humans.

Another interesting point relates to our previous report with islet organoids.¹³ Organoid generation provides the possibility to perfectly control graft size and to include other cell types, in particular endothelial cells, in the structure of the organoid itself. However, this tissue engineering strategy would fall under ATMP regulation due to the extensive islet manipulation. The use of the much simpler shielding method without islet dissociation preserves islet cell mass^{14,15} and could be easily and directly applicable to the clinical situation in a shorter time frame, to improve islet transplant outcome until a more elaborate bioartificial pancreas is designed.

The potential of amniotic membranes to promote angiogenesis and survive without rejection was shown in a previous work, in which allogeneic amniotic membranes were implanted into the peritoneal cavity in a canine model. The authors concluded that their

observation should pave the way for the use of amniotic membranes as immunoisolators for pancreatic islets.³⁶

hAECs immunomodulatory properties have been reported,^{37,38} and previous studies have used approaches similar to the one described herein, combining hAECs with islets to modulate the human alloreactivity in vitro³⁹ and, very recently, in vivo.⁴⁰ This suggests that in addition to enhancing vascularization and engraftment, our strategy could protect the graft from immune reactions, allowing to decrease the strength of immunosuppression regimens. More in vivo studies are still needed to assess the immunological and anti-inflammatory beneficial effect of cotransplanting hAECs with islets in immunocompetent animals.

In summary, the strategy of islet shielding with hAECs enhances islet engraftment through cytoprotective and angiogenic mechanisms. This strategy can improve islet transplant outcomes and allow exploration of new extrahepatic transplant sites before the generation of a more advanced engineered bioartificial pancreas.

ACKNOWLEDGMENTS

This work was supported by grants from the Swiss National Science Foundation (Grant 310030_173138, to Drs Berishvili and Bosco) and from the European Foundation for the Study of Diabetes (to Dr Berishvili). Human islets were provided thanks to a grant from the Juvenile Diabetes Research Foundation (JDRF grant 31-2012-783). The authors thank Thierry Berney for critical review of the manuscript.

DISCLOSURE

The authors of this manuscript have no conflicts of interest to disclose as described by the *American Journal of Transplantation*.

ORCID

Fanny Lebreton  <https://orcid.org/0000-0002-3175-0205>
 Vanessa Lavallard  <https://orcid.org/0000-0001-7328-7549>
 Julie Kerr-Conte  <https://orcid.org/0000-0002-7590-1896>
 François Pattou  <https://orcid.org/0000-0001-8388-3766>
 Ekaterine Berishvili  <https://orcid.org/0000-0002-7969-1937>

REFERENCES

1. Harlan DM, Kenyon NS, Korsgren O, Roep BO. Immunology of Diabetes Society. Current advances and travails in islet transplantation. *Diabetes*. 2009;58(10):2175-2184.
2. Rickels MR, Robertson RP. Pancreatic islet transplantation in humans: recent progress and future directions. *Endocr Rev*. 2019;40(2):631-668.
3. Henriksnas J, Lau J, Zang G, Berggren PO, Kohler M, Carlsson PO. Markedly decreased blood perfusion of pancreatic islets transplanted intraportally into the liver: disruption of islet integrity necessary for islet revascularization. *Diabetes*. 2012;61(3):665-673.
4. Jansson L, Carlsson PO. Pancreatic blood flow with special emphasis on blood perfusion of the islets of Langerhans. *Compr Physiol*. 2019;9(2):799-837.
5. Menger MD, Yamauchi J, Vollmar B. Revascularization and microcirculation of freely grafted islets of Langerhans. *World J Surg*. 2001;25(4):509-515.

6. Carlsson PO, Palm F, Andersson A, Liss P. Markedly decreased oxygen tension in transplanted rat pancreatic islets irrespective of the implantation site. *Diabetes*. 2001;50(3):489-495.
7. Ito T, Itakura S, Todorov I, et al. Mesenchymal stem cell and islet co-transplantation promotes graft revascularization and function. *Transplantation*. 2010;89(12):1438-1445.
8. Kelly Y, Ward C, Duh Q, Chang W, Stock P, Tang Q. Parathyroid CD34+ cells induce neovascularization of donor and recipient leading to chimeric vessel formation and improved engraftment of co-transplanted pancreatic islets. *Am J Transplant*. 2019;19:637.
9. Rackham CL, Chagastelles PC, Nardi NB, Hauge-Evans AC, Jones PM, King AJ. Co-transplantation of mesenchymal stem cells maintains islet organisation and morphology in mice. *Diabetologia*. 2011;54(5):1127-1135.
10. Ward C, Faleo G, Duh Q, et al. Reversal of diabetes and preservation of pancreatic islet grafts in the extrahepatic space with novel parathyroid gland co-transplantation. *Transplantation*. 2018;102:S368-S369.
11. Miki T, Lehmann T, Cai H, Stolz DB, Strom SC. Stem cell characteristics of amniotic epithelial cells. *Stem Cells*. 2005;23(10):1549-1559.
12. Song Y-S, Joo H-W, Park I-H, et al. Transplanted human amniotic epithelial cells secrete paracrine proangiogenic cytokines in rat model of myocardial infarction. *Cell Transplant*. 2015;24(10):2055-2064.
13. Lebreton F, Lavallard V, Bellofatto K, et al. Insulin-producing organoids engineered from islet and amniotic epithelial cells to treat diabetes. *Nat Commun*. 2019;10(1):4491.
14. Callewaert H, Gysemans C, Cardozo AK, et al. Cell loss during pseudoislet formation hampers profound improvements in islet lentiviral transduction efficacy for transplantation purposes. *Cell Transplant*. 2007;16(5):527-537.
15. Kohnert KD, Hehmke B. Preparation of suspensions of pancreatic islet cells: a comparison of methods. *J Biochem Biophys Methods*. 1986;12(1-2):81-88.
16. Ono J, Takaki R, Fukuma M. Preparation of single cells from pancreatic islets of adult rat by the use of dispase. *Endocrinol Jpn*. 1977;24(3):265-270.
17. Borot S, Crowe LA, Parnaud G, et al. Quantification of islet loss and graft functionality during immune rejection by 3-tesla MRI in a rat model. *Transplantation*. 2013;96(5):438-444.
18. Hughes SJ, Bateman PA, Cross SE, et al. Does islet size really influence graft function after clinical islet. *Transplantation?* 2018;102(11):1857-1863.
19. Giuliani M, Moritz W, Bodmer E, et al. Central necrosis in isolated hypoxic human pancreatic islets: evidence for postisolation ischemia. *Cell Transplant*. 2005;14(1):67-76.
20. Lehmann R, Zuellig RA, Kugelmeier P, et al. Superiority of small islets in human islet transplantation. *Diabetes*. 2007;56(3):594-603.
21. Li X, Meng Q, Zhang L. The fate of allogeneic pancreatic islets following intraportal transplantation: challenges and solutions. *J Immunol Res*. 2018;2018:1-13.
22. Ramakrishnan S, Anand V, Roy S. Vascular endothelial growth factor signaling in hypoxia and inflammation. *J Neuroimmune Pharmacol*. 2014;9(2):142-160.
23. Wu Q, Fang T, Lang H, et al. Comparison of the proliferation, migration and angiogenic properties of human amniotic epithelial and mesenchymal stem cells and their effects on endothelial cells. *Int J Mol Med*. 2017;39(4):918-926.
24. Zhu D, Muljadi R, Chan ST, et al. Evaluating the impact of human amniotic epithelial cells on angiogenesis. *Stem Cells Int*. 2016;2016:1-13.
25. Staels W, Heremans Y, Heimberg H, De Leu N. VEGF-A and blood vessels: a beta cell perspective. *Diabetologia*. 2019;62(11):1961-1968.
26. Brady A-C, Martino MM, Pedraza E, et al. Proangiogenic hydrogels within macroporous scaffolds enhance islet engraftment in an extrahepatic site. *Tissue Eng Part A*. 2013;19(23-24):2544-2552.
27. Najjar M, Manzoli V, Abreu M, et al. Fibrin gels engineered with pro-angiogenic growth factors promote engraftment of pancreatic islets in extrahepatic sites in mice. *Biotechnol Bioeng*. 2015;112(9):1916-1926.
28. Su D, Zhang N, He J, et al. Angiopoietin-1 production in islets improves islet engraftment and protects islets from cytokine-induced apoptosis. *Diabetes*. 2007;56(9):2274-2283.
29. Cohen T, Nahari D, Cerem LW, Neufeld G, Levi BZ. Interleukin 6 induces the expression of vascular endothelial growth factor. *J Biol Chem*. 1996;271(2):736-741.
30. Alitalo K, Kurkinen M, Vaheri A, Krieg T, Timpl R. Extracellular matrix components synthesized by human amniotic epithelial cells in culture. *Cell*. 1980;19(4):1053-1062.
31. Parnaud G, Hammar E, Rouiller DG, Armanet M, Halban PA, Bosco D. Blockade of beta1 integrin-laminin-5 interaction affects spreading and insulin secretion of rat beta-cells attached on extracellular matrix. *Diabetes*. 2006;55(5):1413-1420.
32. Sakata N, Goto M, Yoshimatsu G, Egawa S, Unno M. Utility of co-transplanting mesenchymal stem cells in islet transplantation. *World J Gastroenterol*. 2011;17(47):5150-5155.
33. Brissova M, Fowler MJ, Nicholson WE, et al. Assessment of human pancreatic islet architecture and composition by laser scanning confocal microscopy. *J Histochem Cytochem*. 2005;53(9):1087-1097.
34. Dolensek J, Rupnik MS, Stozer A. Structural similarities and differences between the human and the mouse pancreas. *Islets*. 2015;7(1):e1024405.
35. Pingitore A, Ruz-Maldonado I, Liu B, Huang GC, Choudhary P, Persaud SJ. Dynamic profiling of insulin secretion and ATP generation in isolated human and mouse islets reveals differential glucose sensitivity. *Cell Physiol Biochem*. 2017;44(4):1352-1359.
36. Mahgoub MA, Ammar A, Fayed M, et al. Neovascularization of the amniotic membrane as a biological immune barrier. *Transplant Proc*. 2004;36(4):1194-1198.
37. Kolanko E, Kopaczka K, Koryciak-Komarska H, et al. Increased immunomodulatory capacity of human amniotic cells after activation by pro-inflammatory chemokines. *Eur J Pharmacol*. 2019;859:172545.
38. Strom SC, Gramignoli R. Human amnion epithelial cells expressing HLA-G as novel cell-based treatment for liver disease. *Hum Immunol*. 2016;77(9):734-739.
39. Qureshi KM, Oliver RJ, Paget MB, Murray HE, Bailey CJ, Downing R. Human amniotic epithelial cells induce localized cell-mediated immune privilege in vitro: implications for pancreatic islet transplantation. *Cell Transplant*. 2011;20(4):523-534.
40. Zafar A, Lee J, Yesmin S, et al. Rotational culture and integration with amniotic stem cells reduce porcine islet immunoreactivity in vitro and slow xeno-rejection in a murine model of islet transplantation. *Xenotransplantation*. 2019;26(4):e12508.

SUPPORTING INFORMATION

Additional supporting information may be found online in the Supporting Information section.

How to cite this article: Lebreton F, Bellofatto K, Wassmer CH, et al. Shielding islets with human amniotic epithelial cells enhances islet engraftment and revascularization in a murine diabetes model. *Am J Transplant*. 2020;20:1551-1561. <https://doi.org/10.1111/ajt.15812>

Update

American Journal of Transplantation

Volume 20, Issue 12, December 2020, Page 3703

DOI: <https://doi.org/10.1111/ajt.16331>

ERRATUM

In the article by Lebreton et al. (2020),¹ in the section “2.2 Human tissues,” the protocol number in the sentence “Amniotic membranes were harvested from term healthy placentae of woman undergoing elective cesarean section at the Geneva University Hospitals, under CCER protocol 2017-00101” is incorrect.

The protocol number should be CCER protocol 2017-00101 (14-273).

The authors apologize for this error.

REFERENCE

1. Lebreton F, Bellofatto K, Wassmer CH, et al. Shielding islets with human amniotic epithelial cells enhances islet engraftment and revascularization in a murine diabetes model. *Am J Transplant*. 2020;20(6):1551–1561. <https://doi.org/10.1111/ajt.15812>